# *CHAPTER 6*

# DIELECTRIC RELAXATION PHENOMENA AND HIGH FREQUENCY CONDUCTIVITY OF RIGID POLAR LIQUIDS IN DIFFERENT SOLVENTS

## 6.1. Introduction :

Dielectric relaxation studies of polar liquids in non-polar solvents are of much importance as they provide interesting information on solute-solvent and solute-solute molecular formations [6.1-6.2] under high frequency (*hf*) electric field. In order to predict associational aspects of polar liquids one must analyse the measured relaxation parameters to know the relaxation time $\tau$ and the dipole moment $\mu$ of a polar liquid by Cole-Cole [6.3], Cole-Davidson [6.4] plots or by single frequency concentration variation method [6.5].

Srivastava and Srivastava [6.6] studied the relaxation behaviour of chloral and ethyltrichloroacetate in different non-polar solvents under 4.2, 9.8 and 24.6 GHz electric field frequencies from the measured dimensionless dielectric constants like real $k_{ij}'$, imaginary $k_{ij}''$, static $k_{oij}$ and infinite frequency dielectric constant $k_{\infty ij}$ of polar solute (j) in different non-polar solvents (i) at $30^0$C to predict their solute-solvent or solute-solute molecular associations. They, however, inferred that such molecules may possess two or more relaxation processes towards dielectric dispersion phenomena [6.6]. The molecule chloral is widely used in medicine and in the manufacture of D.D.T as insecticide. Ethyltrichloroacetate, on other hand, is used for artificial fragrance of fruits and flowers.

All these facts inspired us to use the measured relaxation data [6.6] for such polar liquids only to detect the double relaxation times $\tau_1$ and $\tau_2$ from the single frequency measurement technique [6.7-6.8]. Earlier investigations have been made on different chain like polar molecules like alcohols in a non-polar solvent [6.9-6.10] to see the double relaxation phenomena at three different electric field frequencies. However, no such study is made so far on such rigid aliphatic polar liquids in different non-polar solvents under various electric field frequencies by the double relaxation formalism derived from single frequency measurements of dielectric relaxation parameters [6.7-6.8]. It is better to study the relaxation phenomena in terms of dimensionless dielectric constants in SI units because of its rationalised coherent and unified nature.

Five systems out of twelve as presented in Table 6.1 show the double relaxation times $\tau_2$ and $\tau_1$ due to rotation of the whole and the flexible parts of the molecule. $\tau_2$ and $\tau_1$ were calculated from the slope and intercept of the linear Eq.(6.7) (see later). All the straight lines are shown graphically in Fig.6.1.

The dipole moments $\mu_2$ and $\mu_1$ of Table 6.2 due to $\tau_2$ and $\tau_1$ were computed in terms of slopes $\beta$'s of total *hf* conductivity $\sigma_{ij}$ against $w_j$ curves of Fig.6.2. All the parabolic curves of conductivities $\sigma_{ij}$'s with $w_j$'s are found to increase with frequency of the electric field.

The calculated $\mu$'s are compared with the theoretical dipole moment $\mu_{theo}$ due to available bond angles and bond moments which are sketched in Fig.6.3 showing the associational aspect of

the polar molecules with solvents to observe the mesomeric and inductive moments in them under *hf* electric field. They are finally compared with the reported $\mu$'s and $\mu_1$ obtained from $\mu_1=\mu_2(c_1/c_2)^{½}$ assuming two relaxation processes are equally probable.

Table 6.1: The estimated relaxation time $\tau_2$ and $\tau_1$ from the slope and the intercept of straight line Eq.(6.5) with errors and correlation coefficients ($r$) together with measured $\tau$ from $\sigma_{ij}''-\sigma_{ij}'$ curve and $\tau_2$'s from single broad dispersion for apparently rigid aliphatic molecules at 30°C under different frequencies of electric fields.

| System with sl. no. & mol. wt.$M_j$ | Frequency $f$ in GHz | Slope and intercept of Eq.(8.3) | | Corrl. coeff. $r$ | % of error in regression technique | Estimated $\tau_2$ and $\tau_1$ in p-sec | | Measured $\tau$ in psec | Reported $\tau$ in psec | $\tau_2$'s in psec from single broad dispersion |
|---|---|---|---|---|---|---|---|---|---|---|
| (I) Chloral | (a) 4.2 | -0.3872 | -0.0732 | -0.91 | 5.54 | 5.27 | - | 4.77 | - | 4.78 |
| in benzene | (b) 9.8 | 3.7238 | 0.5497 | 0.99 | 0.09 | 57.98 | 2.50 | 2.36 | 1.78* | - |
| $M_j$=0.1475 Kg | (c) 24.6 | -0.1936 | -0.2161 | -0.41 | 25.08 | 2.45 | - | 1.73 | - | 2.01 |
| (II) Chloral | (a) 4.2 | -2.7611 | -0.4191 | -0.78 | 12.81 | 5.44 | - | 3.74 | - | 40.87 |
| in *n*-heptane | (b) 9.8 | 1.6593 | 0.1040 | 0.93 | 3.89 | 25.89 | 1.06 | 1.82 | 0.46* | - |
| $M_j$=0.1475 Kg | (c) 24.6 | 1.7458 | 0.1752 | 0.95 | 2.56 | 10.60 | 0.69 | 0.91 | - | - |
| (III) Ethyltri- | (a) 4.2 | 0.3545 | -0.0699 | 0.37 | 23.75 | 18.78 | - | 23.00 | - | 18.71 |
| chloroacetate | (b) 9.8 | 1.5123 | -0.1797 | 0.96 | 1.87 | 26.36 | - | 7.28 | 6.50** | 32.53 |
| in benzene $M_j$=0.1915 Kg | (c) 24.6 | -2.7470 | -3.3227 | -0.24 | 25.86 | 5.88 | - | 3.34 | - | 37.19 |
| (IV) Ethyltri- | (a) 4.2 | -1.7251 | -0.9325 | -0.26 | 25.68 | 16.38 | - | 16.53 | - | 20.13 |
| chloroacetate | (b) 9.8 | 1.5182 | 0.0549 | 0.66 | 15.40 | 24.05 | 0.60 | 6.28 | 5.70** | - |
| in *n*-hexane $M_j$=0.1915 Kg | (c) 24.6 | 2.9891 | 1.6141 | 0.98 | 0.83 | 14.76 | 4.58 | 5.76 | - | - |

*= Cole-Cole plot **= Gopalakrishna's method

The relative contributions $c_1$ and $c_2$ towards dielectric dispersions for the five systems were obtained from the theoretical values of $x=(k_{ij}'-k_{\infty ij})/(k_{oij}-k_{\infty ij})$ and $y=k_{ij}''/(k_{oij}-k_{\infty ij})$ of Fröhlich's theory [6.11] in terms of estimated $\tau_2$ and $\tau_1$ of Table 6.1. They were also computed from the values of $x$ and $y$ at $w_j\rightarrow 0$ of graphical technique [6.7-6.8] and placed in Table 6.3 for comparison with Fröhilch's $c_1$ and $c_2$. The variations of $x$ and $y$ with $w_j$ of solute of Figs.6.4 and 6.5 are the least squares fitted parabolae with the experimental data. They are of convex and concave shapes except ethyltrichloroacetate in *n*-hexane at 9.8 and 24.6 GHz electric fields. This sort of behaviours was not observed earlier [6.7-6.8]. With these values of $x$ and $y$ at $w_j\rightarrow 0$ the symmetric and asymmetric distribution parameters $\gamma$ and $\delta$ of the molecules at those frequencies are computed and are placed in Table 6.3 to indicate the non-rigidity of the molecules in *hf* electric field.

## 6.2. Theoretical Formulations :

Assuming the molecules to possess two separate board dispersions under *hf* electric field. Bergmann equations [6.12] are:

$$\frac{k'_{ij}-k_{\infty ij}}{k_{oij}-k_{\infty ij}} = c_1\frac{1}{1+\omega^2\tau_1^2}+c_2\frac{1}{1+\omega^2\tau_2^2} \qquad \ldots\ldots(6.1)$$

$$\frac{k''_{ij}}{k_{oij}-k_{\infty ij}} = c_1\frac{\omega\tau_1}{1+\omega^2\tau_1^2}+c_2\frac{\omega\tau_2}{1+\omega^2\tau_2^2} \qquad \ldots\ldots(6.2)$$

such that the sum of the relative weight factors $c_1$ and $c_2$ towards dielectric dispersion is unity i.e $c_1+c_2=1$.

Table 6.2: Estimated intercept and slope of $\sigma_{ij}$–$w_j$ equations, dimensionless parameters $b_2$, $b_1$ [Eq.(6.13)], estimated dipole moments $\mu_2$, $\mu_1$ from Eq.(6.12) and $\mu_{theo}$ from bond angles and bond moment together with $\mu_1$ from $\mu_1=\mu_2(c_1/c_2)^{1/2}$ and reported $\mu$ in Coulomb.metre (C.m).

| System with sl. no. & mol. wt.$M_j$ | $f$ in GHz | Intercept & slope of $\sigma_{ij}$–$w_j$ equation | | Dimensionless parameter | | Estimated $\mu X10^{30}$ in C.m | | Reported $\mu X10^{30}$ in C.m | Estimated $\mu_1 X10^{30}$ in C.m from $\mu_1=\mu_2(c_1/c_2)^{1/2}$ | $\mu_{theo}$ in C.m |
|---|---|---|---|---|---|---|---|---|---|---|
| | | $\alpha$ | $\beta$ | $b_1$ | $b_2$ | $\mu_2$ | $\mu_1$ | | | |
| (I) Chloral | 4.2 | 5.990 | 4.208 | - | 0.981 | 5.02 | - | 5.01* | - | |
| in benzene | 9.8 | 13.791 | 10.800 | 0.977 | 0.073 | 19.32 | 5.27 | 4.87** | 13.26 | 10.02 |
| $M_j$=0.1475 Kg | 24.6 | 34.880 | 26.010 | - | 0.875 | 5.46 | - | 5.28* | - | |
| (II) Chloral | 4.2 | 5.058 | 3.619 | - | 0.980 | 5.78 | - | 5.72* | - | |
| in *n*-heptane | 9.8 | 11.772 | 6.001 | 0.996 | 0.282 | 9.07 | 4.83 | 6.00** | 9.71 | 10.02 |
| $M_j$=0.1475 Kg | 24.6 | 29.631 | 16.513 | 0.989 | 0.271 | 9.69 | 5.08 | 5.10* | 9.63 | |
| (III) Ethyltri- | 4.2 | 5.990 | 9.057 | - | 0.803 | 9.27 | - | 9.72* | - | |
| chloroacetate | 9.8 | 14.100 | 10.334 | - | 0.275 | 11.07 | - | 6.50** | - | 10.50 |
| in benzene | 24.6 | 34.188 | 39.357 | - | 0.548 | 9.67 | - | 8.05* | - | |
| $M_j$=0.1915 Kg | | | | | | | | | | |
| (IV) Ethyltri- | 4.2 | 4.984 | 5.599 | - | 0.843 | 8.97 | - | 8.99* | - | |
| chloroacetate | 9.8 | 11.522 | 12.722 | 0.999 | 0.313 | 14.53 | 8.14 | 8.67** | 17.15 | 10.50 |
| in *n*-hexane | 24.6 | 28.160 | 36.525 | 0.666 | 0.161 | 21.66 | 10.65 | 11.64* | 16.37 | |
| $M_j$=0.1915 Kg | | | | | | | | | | |

** Ref [6.5] *Computed from conductivity

Solving Eqs.(6.1) and (6.2) for $c_1$ and $c_2$ one gets:

$$c_1 = \frac{(x\alpha_2 - y)(1+\alpha_1^2)}{\alpha_2-\alpha_1} \qquad \ldots\ldots(6.3)$$

$$c_2 = \frac{(y - x\alpha_1)(1+\alpha_2^2)}{\alpha_2-\alpha_1} \qquad \ldots\ldots(6.4)$$

where $x = (k_{ij}' - k_{\infty ij})/(k_{oij} - k_{\infty ij})$ and $y = k_{ij}''/(k_{oij} - k_{\infty ij})$. The term $\alpha = \omega\tau$ and suffices 1 and 2 are, however, related to $\tau_1$ and $\tau_2$ respectively. Adding Eqs.(6.3) and (6.4) one gets:

$$\frac{k_{oij} - k_{ij}'}{k_{ij}' - k_{\infty ij}} = \omega(\tau_1 + \tau_2)\frac{k_{ij}''}{k_{ij}' - k_{\infty ij}} - \omega^2\tau_1\tau_2 \qquad \ldots\ldots (6.5)$$

as a linear equation having intercept $-\omega^2\tau_1\tau_2$ and slope $\omega(\tau_1+\tau_2)$ which are obtained from the measured dielectric constants at different $w_j$'s of solutes under a single frequency electric field at a given temperature by applying linear regression technique and $\omega$= the angular frequency $=2\pi f$, $f$ being the frequency in GHz.

Assuming a single broad Debye like dispersion for the polar molecules the Eq.(6.5) is reduced to the from [6.8] with $\tau_1=0$.

$$\frac{k_{oij} - k_{ij}'}{k_{ij}' - k_{\infty ij}} = \omega\tau_2 \frac{k_{ij}''}{k_{ij}' - k_{\infty ij}} \qquad \ldots\ldots (6.6)$$

in order to get $\tau_2$ for seven polar-nonpolar liquid mixtures placed in the 11th column Table 6.1.

Again, the complex *hf* conductivity $\sigma_{ij}^*$ is related to $k_{ij}'$ and $k_{ij}''$ by the relation:

$$\sigma_{ij}^* = \sigma_{ij}' + j\sigma_{ij}''$$

where $\sigma_{ij}' = \omega\varepsilon_o k_{ij}''$ and $\sigma_{ij}'' = \omega\varepsilon_o k_{ij}'$ are the real and imaginary parts of the complex conductivity $\sigma_{ij}^*$. The magnitude of total *hf* conductivity is given by:

$$\sigma_{ij} = \omega\varepsilon_o (k_{ij}''^2 + k_{ij}'^2)^{1/2} \qquad \ldots\ldots (6.7)$$

$\sigma_{ij}''$ is related to $\sigma_{ij}'$ by the relation:

$$\sigma_{ij}'' = \sigma_{\infty ij} + \frac{1}{\omega\tau_j}\sigma_{ij}' \qquad \ldots\ldots (6.8)$$

where $\tau_j$ is the measured relaxation time of a polar unit and $\sigma_{\infty ij}$ is constant conductivity at $w_j \to 0$.

In the *hf* region, total conductivity $\sigma_{ij} \cong \sigma_{ij}''$, hence Eq.(6.8) is written as:

$$\sigma_{ij} = \sigma_{\infty ij} + \frac{1}{\omega\tau_j}\sigma_{ij}'$$

$$\left(\frac{d\sigma_{ij}}{dw_j}\right)_{w_j \to 0} = \frac{1}{\omega\tau_j}\left(\frac{d\sigma_{ij}'}{dw_j}\right)_{w_j \to 0}$$

$$\beta = \frac{1}{\omega\tau_j}\left(\frac{d\sigma_{ij}'}{dw_j}\right)_{w_j \to 0} \qquad \ldots\ldots (6.9)$$

The real part of *hf* conductivity $\sigma_{ij}'$ at $T$ K for $w_j$ of a solute is [6.13-6.14]:

$$\sigma_{ij}' = \frac{N\rho_{ij}\mu_j^2}{27k_BTM_j}\left(\frac{\omega^2\tau_j}{1+\omega^2\tau_j^2}\right)(k_{ij}'+2)^2 w_j \qquad \ldots\ldots (6.10)$$

On differentiation with respect to $w_j$ and at $w_j \to 0$, Eq.(6.10) becomes:

$$\left(\frac{d\sigma_{ij}'}{dw_j}\right)_{w_j\to 0} = \frac{N\rho_i\mu_j^2}{27k_BTM_j}\left(\frac{\omega^2\tau_j}{1+\omega^2\tau_j^2}\right)(k_i+2)^2 \qquad \ldots\ldots (6.11)$$

where all the symbols expressed is S I units carry usual meanings [6.14]. From Eqs.(6.9) and (6.11) one gets *hf* dipole moment $\mu_j$ from:

$$\mu_j = \left(\frac{27k_BTM_j}{N\rho_i(k_i+2)^2}\frac{\beta}{\omega b}\right)^{1/2} \qquad \ldots\ldots (6.12)$$

The dimensionless parameter $b$ is related to $\tau$ by:

$$b = \frac{1}{1+\omega^2\tau_j^2} \qquad \ldots\ldots (6.13)$$

all the $\mu_j$'s, $b$'s and $\beta$'s as computed for chloral and ethyltrichloroacetate are presented in Table 6.2.

Table 6.3: Fröhlich parameter $A$ [$=\ln(\tau_2/\tau_1)$], relative contributions $c_1$ and $c_2$ due to $\tau_1$ and $\tau_2$, theoretical values of $x$ and $y$ from Fröhlich Eqs.(6.14) and (6.15) and from fitting equations as shown in Figs.6.4 and 6.5 at $w_j \to 0$ and symmetric and asymmetric distribution parameters $\gamma$ and $\delta$ for the five polar-nonpolar liquid mixtures at 30°C.

| System with sl. no. | $f$ in GHz | A | Theoretical values of $x$ and $y$ from Eqs. (6.14) & (6.15) | | Theoretical values of $c_1$ and $c_2$ | | Estimated values of $x$ and $y$ at $w_j \to 0$ | | Estimated values of $c_1$ and $c_2$ | | Estimated values of $\gamma$ and $\delta$ | |
|---|---|---|---|---|---|---|---|---|---|---|---|---|
| (I) Chloral in benzene | 9.8 | 3.14 | 0.587 | 0.364 | 0.52 | 1.10 | 0.362 | 0.228 | 0.32 | 0.69 | 0.42 | 0.38 |
| (II) Chloral in *n*-heptane | 9.8 | 3.12 | 0.803 | 0.296 | 0.65 | 0.56 | 0.610 | 0.318 | 0.43 | 0.64 | 0.26 | 0.42 |
| | 24.6 | 2.73 | 0.763 | 0.336 | 0.60 | 0.61 | 0.671 | 0.287 | 0.54 | 0.52 | 0.29 | 0.35 |
| (IV) Ethyltri-chloroacetate in *n*-hexane | 9.8 | 3.69 | 0.843 | 0.255 | 0.69 | 0.49 | 0.446 | 0.284 | 0.26 | 0.59 | 0.34 | 0.42 |
| | 24.6 | 1.17 | 0.394 | 0.463 | 0.42 | 0.73 | -0.327 | 0.383 | -1.07 | 2.41 | -0.62 | – |

The molecules under consideration are of complex type and only a few data are available under single frequency measurement. In the case of a continuous distribution of $\tau$'s between the two

extreme values [6.12] of $\tau_1$ and $\tau_2$, Fröhlich's theory [6.11] based on distribution of $\tau$ yields:

$$x = \frac{k'_{ij} - k_{\infty ij}}{k_{oij} - k_{\infty ij}} = 1 - \frac{1}{2A} \ln\left(\frac{1+\omega^2\tau_2^{\,2}}{1+\omega^2\tau_1^{\,2}}\right) \qquad \ldots\ldots (6.14)$$

$$y = \frac{k''_{ij}}{k_{oij} - k_{\infty ij}} = \frac{1}{A}\left[\tan^{-1}(\omega\tau_2) - \tan^{-1}(\omega\tau_1)\right] \qquad \ldots\ldots (6.15)$$

where $A$=Fröhlich parameter=$\ln(\tau_2/\tau_1)$. The theoretical values of $x$ and $y$ of Eqs.(6.14) and (6.15) were used to get $c_1$ and $c_2$. The values of $c_1$ and $c_2$ can be had from the graphical plots of $x$ and $y$ at $w_j \to 0$ as seen in Figs.6.4 and 6.5 respectively. $c_1$ and $c_2$ thus obtained by both the methods are shown in Table 6.3 for comparison.

The molecules under five different environments show double relaxation phenomena (Table 6.1) indicating their non-rigidity. In such cases dielectric relaxation behaviour may be represented by [6.3-6.4]:

$$\frac{k^*_{ij} - k_{\infty ij}}{k_{oij} - k_{\infty ij}} = \frac{1}{1+(j\omega\tau_s)^{1-\gamma}} \qquad \ldots\ldots (6.16)$$

$$\frac{k^*_{ij} - k_{\infty ij}}{k_{oij} - k_{\infty ij}} = \frac{1}{(1+j\omega\tau_{cs})^{\delta}} \qquad \ldots\ldots (6.17)$$

where $\gamma$ and $\delta$ are symmetric and asymmetric distribution parameters which are, however, related to symmetric and characteristic relaxation times $\tau_s$ and $\tau_{cs}$ respectively.

Separating the real and the imaginary parts from Eq.(6.16) we have,

$$\gamma = \frac{2}{\pi}\tan^{-1}\left[(1-x)\frac{x}{y} - y\right] \qquad \ldots\ldots (6.18)$$

where $x = (k_{ij}' - k_{\infty ij})/(k_{oij} - k_{\infty ij})$ and $y = k_{ij}''/(k_{oij} - k_{\infty ij})$ are obtained at $w_j \to 0$ from Figs.6.4 and 6.5 respectively. Similarly, $\delta$ can be calculated as:

$$\tan(\phi\delta) = \frac{y}{x} \qquad \ldots\ldots (6.19)$$

$$\log(\cos\phi)^{1/\phi} = \frac{\log(x/\cos\phi\delta)}{\phi\delta} \qquad \ldots\ldots (6.20)$$

where $\tan\phi = \omega\tau_{cs}$. To get $\delta$, a theoretical curve of $\log(\cos\phi)^{1/\phi}$ against $\phi$ is drawn as seen in Fig.6.6. Knowing $\delta\phi$ from Eq.(6.19), $\phi$ can be found out from curve of Fig.6.6. With the known $\phi$, $\delta$ can be estimated. $\gamma$ and $\delta$ are entered in the 12th and 13th columns of Table 6.3.

## 6.3. Results and Discussions :

Fig.6.1 showed the linear variation of $(k_{oij}-k_{ij}')/(k_{ij}'-k_{\infty ij})$ against $k_{ij}''/(k_{ij}'-k_{\infty ij})$ for different $w_j$'s of chloral and ethyltrichloroacetate in different non-polar solvents under 4.2, 9.8 and 24.6 GHz electric field frequencies at 30°C. The linearity is expressed in terms of correlation coefficients $r$'s as seen in Table 6.1. The percentage of errors in terms of $r$'s in the regression technique were calculated in order to place them in Table 6.1. The estimated values of $\tau_2$ and $\tau_1$ from intercepts and slopes of Eq.(6.5) are shown in the 7th and 8th columns of Table 6.1. Double relaxation phenomena are, however, observed for chloral in $n$-heptane and ethyltrichloroacetate in $n$-hexane at 9.8 and 24.6 GHz electric fields. Chloral in benzene at 9.8 GHz also showed the same phenomenon. This observation reveals that the probability of showing double relaxation phenomena in aliphatic non-polar solvents at higher frequencies is maximum for such rigid aliphatic polar liquids. The electrostatic interaction of polar molecules with $\pi$-delocalised electron cloud of $C_6H_6$ – ring increases the rigidity to show $\tau_2$ only for the whole molecular rotation. The interaction appears to be absent for aliphatic polar liquids in alicyclic aliphatic non-polar solvents and thus the double relaxation times $\tau_2$ and $\tau_1$ are seen to occur in higher frequencies for their flexibility. Chloral in $C_6H_6$ at 9.8 GHz is exception probably due to the fact that the effective dispersive region [6.15] lies near 10 GHz electric field for such systems. $\tau_2$'s for the rest seven systems showing single relaxation phenomena were also calculated assuming single broad Debye like dispersion [6.8] in them. They are placed in the 11th column of Table 6.1. It is interesting to note that $\tau_1$'s for the five systems agree well with the measured $\tau$ from Eq.(6.8) of conductivity measurement. This fact shows that *hf* conductivity measurement always yields the average microscopic $\tau$ whereas the double relaxation phenomena offer a better understanding of microscopic as well macroscopic molecular $\tau$

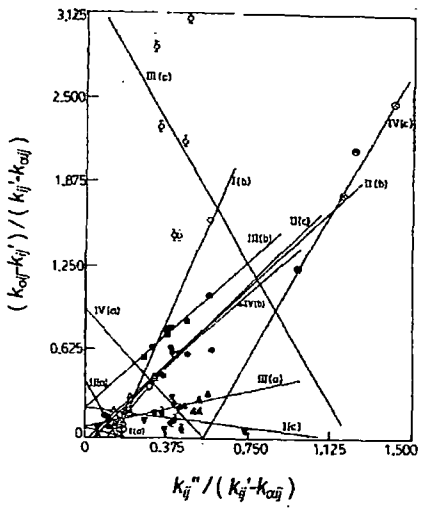


Figure 6.1: Linear variation of $(k_{oij}-k_{ij}')/(k_{ij}'-k_{\infty ij})$ against $k_{ij}''/(k_{ij}'-k_{\infty ij})$ for different $w_j$'s at 30°C. I(a), I(b) and I(c) for chloral in benzene (⧗, ○ , ▼ ); II(a), II(b) and II(c) for chloral in $n$-heptane ( ◑ Δ, □ ); III(a), III(b) and III(c) for ethyltrichloroacetate in benzene ( ▲ , ■ , ⬙ ); IV(a), IV(b) and IV(c) for ethyltrichloroacetate in $n$-hexane ( ◆, ●, ⊕ ,) under 4.2, 9.8 and 24.6 GHz electric fields respectively

as observed elsewhere [6.9]. $\tau_2$ of Table 6.1 is higher at 9.8 GHz and decrease gradually both at 4.2 GHz and 24.6 GHz electric fields in different solvents. This type of behaviour is probably due to larger size of the rotating unit in the effective dispersive region of nearly 10 GHz due to solute-solvent or solute-solute molecular associations which break up with the increase or decrease from nearly 10 GHz electric field frequency. All the $\tau$ and $\tau_1$ agree well with the available reported $\tau$ placed in the 10th column of Table 6.1 establishing the fact that the rotation of a part of the molecule is possible under *hf* electric field [6.16].

The dipole moments $\mu_2$ and $\mu_1$ of the polar molecules were calculated in terms of dimensionless parameters $b$'s involved with $\tau$'s of Eq.(6.13) and slope $\beta$ of $\sigma_{ij}$–$w_j$ curve of Fig.6.2 as seen in Table 6.2. The polar liquid in a given non-polar solvent behaves as a bound charged species due to polarisation under GHz electric field in order to have large *hf* conductivity $\sigma_{ij}$ for different $w_j$ although they are insulators. The parabolic variation of $\sigma_{ij}$ with $w_j$ increases with the electric field frequency as found in Fig.6.2 yielding different slopes $\beta$'s which are usually used to calculate *hf* $\mu_j$ of a polar liquid from Eqs.(6.12) and (6.13) at a given temperature. $\mu_2$'s are found to increase from 4.2 GHz electric fields for chloral in *n*-heptane and ethyltrichloroacetate in *n*-hexane. This type of behaviour is probably due to rupture of solute-solute and solute-solvent molecular association in the *hf* electric field and the corresponding increase in the absorbtion for smaller molecular species [6.17]. But chloral and ethyltrichloroacetate in benzene show higher values of $\mu_2$ at 9.8 GHz and decrease gradually from 24.6 GHz to 4.2 GHz electric fields. Such type of behaviour may be due to strong absorbtion of electric energy at 9.8 GHz and solute-solvent association of the polar solute with benzene ring. $\mu_2$ and $\mu_1$ are, however, compared with the $\mu_{theo}$'s due to available bond angles and bond moments $8.0\times10^{-30}$, $5.0\times10^{-30}$, $0.3\times10^{-30}$ and $2.4\times10^{-30}$ Coulomb-metre for >C⇐O, C←Cl, C←C and C→$OCH_3$ (making an angle $57^0$ with bond axis ) respectively as displayed in Fig.6.3. $\mu_{theo}$'s are

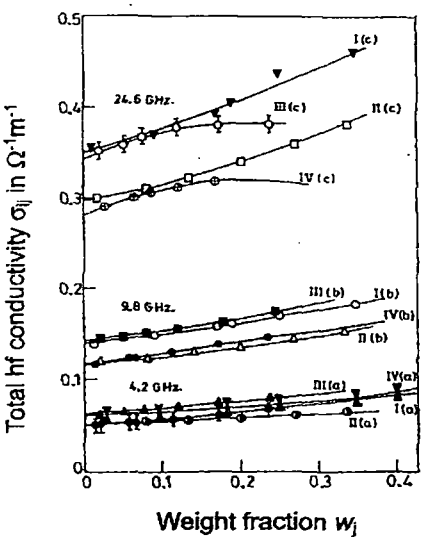


Figure 6.2: Total *hf* conductivity $\sigma_{ij}$ in $\Omega^{-1}m^{-1}$ against $w_j$'s at $30^0$C. I(a), I(b) and I(c) for chloral in benzene (⧗, O , ▼ ); II(a), II(b) and II(c) for chloral in *n*-heptane (◑,Δ, □ ); III(a), III(b) and III(c) for ethyltrichloroacetate in benzene ( ▲ , ■ ,◊ ); IV(a), IV(b) and IV(c) for ethyltrichloroacetate in *n*-hexane (◆, ●,⊕ ,) under 4.2, 9.8 and 24.6 GHz electric fields respectively

placed in the 11th column of Table 6.2. The molecule chloral shows slightly larger $\mu_{theo}$ probably due to solute-solute molecular associations [Fig.6.3(ii)] in the comparatively concentrated solution as expected. The solute-solute associations may arise due to interaction of fractional positive charge $\delta^+$ on C-atom and negative charge $\delta^-$ on O-atom of >C⇐O group between two solute molecules.

The solute-solvent association with benzene is explained on the basis of the interaction between C

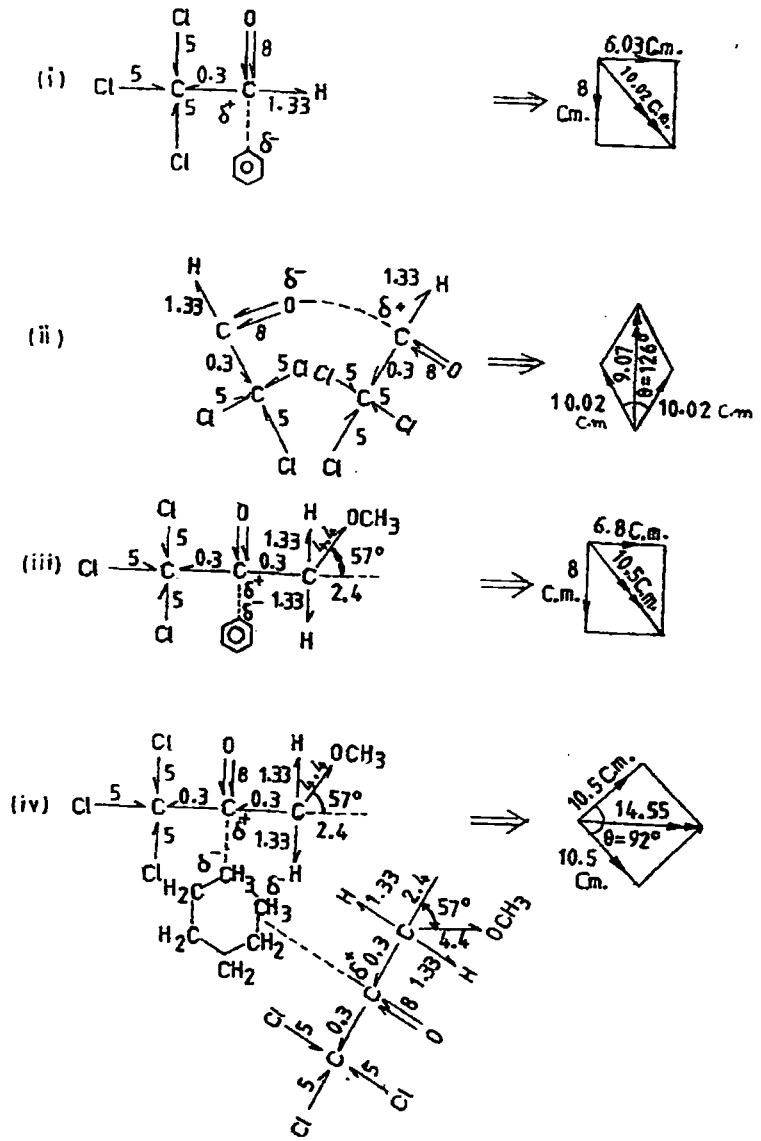


Figure 6.3: Conformational structures of chloral and ethyltrichloroacetate from bond angles and bond moments in multiple of $10^{-30}$ Coulomb.metre.

(i) Solute-solvent association of chloral in benzene; (ii) Solute-solute association of chloral; (iii) Solute-solvent association of ethyltrichloroacetate in benzene and (iv) Solute-solute association of ethyltrichloroacetate in *n*-hexane.

atom of >C⇐O group and $\pi$-delocalised electron cloud of $C_6H_6$ ring. Ethyltrichloroacetate, on the other hand, shows $\mu_{theo}$ in agreement with the estimated $\mu_j$'s in $C_6H_6$. This is due to solute-solvent association as sketched in Fig.6.3[(i) and (iii)] which confirms the orientation of the bond angles and bond moments of the substituents polar groups of the molecules in $C_6H_6$. The slight disagreement between the observed and theoretical $\mu$'s may be either due to the steric hindrances or the mesomeric, inductive and electromeric effects existing within the polar groups attached to the parent ones. Larger values of measured $\mu_j$'s invariably suggest the solute-solute interactions in alicyclic solvent *n*-hexane due to interaction between adjacent C and O atoms of >C⇐O groups of two molecules as shown in Fig.6.3 [(ii) and (iv)]. However, the reduced bond moments by $\mu_j/\mu_{theo}$'s in agreement with the estimated $\mu_j$'s reveals the mesomeric, inductive and electromeric effects within the polar groups of the molecules under consideration.

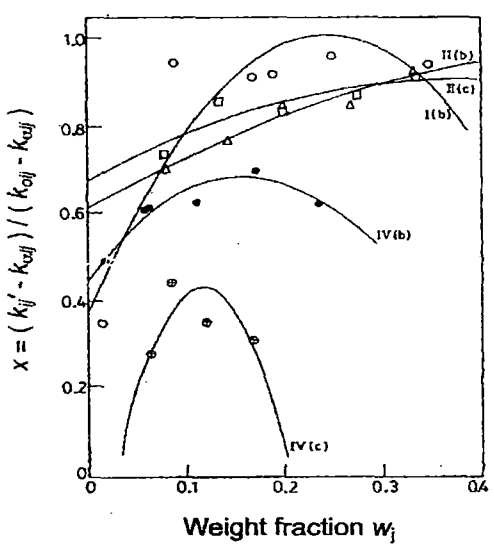


Figure 6.4: Variation of $x = (k_{ij}' - k_{\alpha ij})/(k_{oij} - k_{\alpha ij})$ with $w_j$'s of chloral and ethyltrichloroacetate at 30°C
I(b) for chloral in benzene at 9.8 GHz ( O ); II(b) and II(c) for chloral in *n*-heptane at 9.8 and 24.6 GHz ( Δ, □ ); IV(b) and IV(c) for ethyltrichloroacetate in *n*-hexane at 9.8 and 24.6 GHz (●, ⊕ ) electric fields.

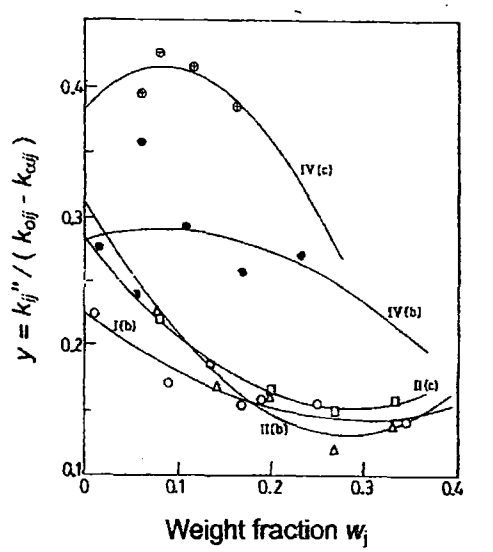


Figure 6.5: Variation of $y = k_{ij}''/(k_{oij} - k_{\alpha ij})$ with $w_j$'s of chloral and ethyltrichloroacetate at 30°C
I(b) for chloral in benzene at 9.8 GHz ( O ); II(b) and II(c) for chloral in *n*-heptane at 9.8 and 24.6 GHz ( Δ, □ ); IV(b) and IV(c) for ethyltrichloroacetate in *n*-hexane at 9.8 and 24.6 GHz (●, ⊕) electric fields

The relative contributions $c_1$ and $c_2$ toward dielectric dispersions due to $\tau_1$ and $\tau_2$ are, however, calculated from $x = (k_{ij}' - k_{\alpha ij})/(k_{oij} - k_{\alpha ij})$ and $y = k_{ij}''/(k_{oij} - k_{\alpha ij})$ of Eqs.(6.14) and (6.15) of Fröhlich's methods [6.11]. They are compared with those due to $x$ and $y$ from graphical methods

of Figs.6.4 and 6.5 at $w_j \to 0$. Both the methods yield $c_1+c_2 \cong 1$ suggesting the applicability of the methods. The nature of variation of $x$ and $y$ with $w_j$ is convex and concave (except ethyltrichloroacetate in *n*-hexane at 9.8 GHz and 24.6 GHz) which is not usual as observed earlier [6.7-6.8]. Such type of behaviour explained that unlike increase of $\tau$ [6.18] it decreases with $w_j$ probably due to solute-solute and solute-solvent molecular association. All the values of $c_1$ and $c_2$ are placed in Table 6.3 for comparison. In order to test the rigidity of the molecules the symmetric and asymmetric distribution parameter $\gamma$ and $\delta$ were estimated from Eqs.(6.18) and (6.19) for fixed values of $x$ and $y$ at $w_j \to 0$ of Figs.6.4 and 6.5. The values of $\log(\cos\phi)^{1/\phi}$ against $\phi$ in degree as shown in Fig.6.6 is essential to get $\delta$. Knowing $\phi$ from the curve of Fig.6.6, $\delta$'s were obtained. Both $\gamma$ and $\delta$ are placed in Table 6.3. The values of $\gamma$ establish the fact that the molecules obey the symmetric relaxation phenomena as $\delta$'s are very low [6.19].

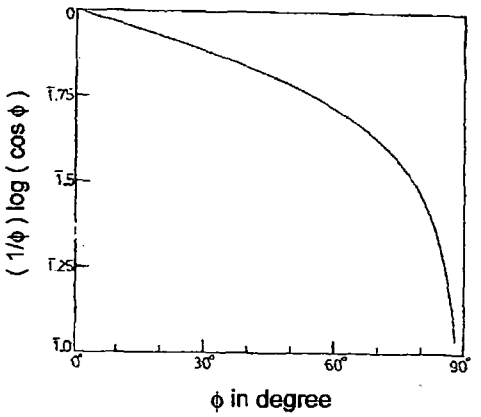


Figure 6.6: Plot of $(1/\phi)\log(\cos\phi)$ against $\phi$ in degree

### 6.4. Conclusions :

The study of dielectric relaxation mechanism by dimensionless dielectric constants gives a new insight into polar-polar and polar-nonpolar molecular interactions. The single frequency measurement of dielectric relaxation parameters provides a unique method to get macroscopic and microscopic relaxation times $\tau_2$ and $\tau_1$ and hence dipole moments $\mu_2$ and $\mu_1$ of the whole and the flexible part of the molecule. The estimation of $\tau_j$ or $\tau_1$ and $\tau_2$ from a linear equation is very simple and straightforward to get $\mu_j$ or $\mu_1$ and $\mu_2$ in terms of slope of $\sigma_{ij}$–$w_j$ curve. The errors in measurement of $\tau_j$ and $\mu_j$ can be computed by correlation coefficients and are claimed to be accurate within 10% and 5% respectively. The molecules under different states of environment show interesting phenomena of double or single relaxation mechanism. When the solute-solvent molecular interaction is almost absent in the polar solute in alicyclic aliphatic solvent; flexible part along with the whole molecule rotates under *hf* electric field giving rise what is known as double relaxation. The solute-solvent association, on the other hand, favours the existence of single relaxation phenomena by the whole molecular rotations as $\pi$-delocalised electron clouds of solvent interact

with the flexible parts to cease their rotations. The probability of showing double relaxation is, thus greater in aliphatic solvents. Various types of molecular associations like solute-solute and solute-solvent interactions are inferred from departure of the graphical plots of $x = (k_{ij}' - k_{\infty ij})/(k_{oij} - k_{\infty ij})$ and $y = k_{ij}''/(k_{oij} - k_{\infty ij})$ with $w_j$ of Bergmann's equations. Nonrigid characteristics of the molecules are confirmed by estimation of symmetric $\gamma$ and asymmetric distribution parameter $\delta$. The molecular associations are also supported by the conformational structures of the molecules in which the presence of mesomeric, inductive and electromeric moments due to >C⇐O group are found to play their vital role. The correlation between the conformational structures of such polar liquids with the observed results enhances the scientific content of the paper in order to add a better understanding of the existing knowledge of dielectric relaxation phenomena.

**References :**


[6.1] A K Sharma, D R Sharma and D S Gill, *J. Phys. D: Appl. Phys.* **18** 1199 (1985)

[6.2] A Sharma and D R Sharma, *J. Phys. Soc. Japan* **61** 1049 (1992)

[6.3] K S Cole and R H Cole, *J. Chem. Phys.* **9** 341 (1941)

[6.4] D W Davidson and R H Cole, *J. Chem. Phys.* **19** 1484 (1951)

[6.5] K V Gopalakrishna, *Trans. Faraday Soc.* **53** 767 (1957)

[6.6] S K Srivastava and S L Srivastava, *Indian J. Pure & Appl. Phys.* **13** 179 (1975)

[6.7] U Saha, S K Sit, R C Basak and S Acharyya, *J. Phys. D: Appl. Phys.* **27** 596 (1994)

[6.8] S K Sit, R C Basak, U Saha and S Acharyya, *J. Phys. D: Appl. Phys.* **27** 2194 (1994)

[6.9] S K Sit and S Acharyya, *Indian J. Phys.* **70B** 19 (1996)

[6.10] S K Sit, N Ghosh and S Acharyya, *Indian J. Pure & Appl. Phys.* **35** 329 (1997)

[6.11] H Frohlich, *Theory of Dielectrics* (Oxford University Press) p.94 (1949)

[6.12] K Bergmann, D M Roberti and C P Smyth, *J. Phys. Chem.* **64** 665 (1960)

[6.13] C P Smyth, *Dielectric Behaviour and Structure* (New York: McGraw Hill) (1955)

[6.14] R C Basak, A K Karmakar, S K Sit and S Acharyya, *Indian J. Pure & Appl. Phys.* **37** 224 (1999)

[6.15] S K Sit and S Acharyya, *Indian J. Pure & Appl. Phys.* **34** 255 (1996)

[6.16] R C Basak, S K Sit, N Nandi and S Acharyya, *Indian J. Phys.* **70B** 37 (1996)

[6.17] L Glasser, J Crossley and C P Smyth, *J. Chem. Phys.* **57** 3977 (1972)

[6.18] S N Sen and R Ghosh, *Indian J. Pure & Appl. Phys.* **10** 701 (1972)

[6.19] S Chandra and J Prakash, *J. Phys. Soc. Japan* **35** 876 (1975)